



PREPARATION AND STUDY OF THE PHYSICAL PROPERTIES OF SOME COMPLEXES WITH SCHIFF BASE LIGAND FOR CEFIDINIR DERIVATIVE

Haneen R. Ali¹, Sahar S. Hassan²

¹Researcher, Department of Chemistry, College of Science for Women, University of Baghdad, Baghdad, Iraq. hanein.rafiel205a@csw.uobaghdad.edu.iq

²Assistant Professor PhD., Department of Chemistry, College of Science for Women, University of Baghdad, Baghdad, Iraq. saharsabeeh21@yahoo.com

Received 7/ 8/ 2022, Accepted 10/ 10/ 2022, Published 31/ 12/ 2022

This work is licensed under a CC BY 4.0 <https://creativecommons.org/licenses/by/4.0>



ABSTRACT

Metal (II) complexes of Co, Ni, Cu and Zn with cefdinir $C_{14}H_{13}N_5O_5S_2$ derivative (L) were synthesized and identification by elemental analysis CHNS Uv-Vis, FTIR, TGA, metal analysis AA, magnetic susceptibility and conduct metric measurement. by analysis the ligand behaves as a bidentate. For the cobalt complex, Tetrahedral geometry shape was suggested, while other complexes that have nickel, copper and zinc ions were proposed as octahedral geometry shape. The experimental method was studied for prevention of corrosion carbon steel in 3.5% NaCl by using a novel Cefdinir derivations drugs. The results showed that metal complex was a strong corrosion resistance protect for carbon steel in sodium chloride and the inhibition efficiency (%) increased with increasing concentration of drugs due to that the novel Cefdinir derivative drugs metal complex was adsorpd from saline solution on surface of carbon steel.

Keywords: Corrosion resistance, elemental analysis CHNS, Uv-Vis and FTIR spectroscopies, cefdinir derivative.

تحضير ودراسة الخواص الفيزيائية لبعض معقدات ليكاند قاعدة شيف لمشتق Cefdinir

حنين رافع علي¹، سحر صبيح حسن²

¹باحثة، قسم الكيمياء، كلية العلوم للبنات، جامعة بغداد، بغداد، العراق. hanein.rafiel205a@csw.uobaghdad.edu.iq

²استاذ مساعد دكتور، قسم الكيمياء، كلية العلوم للبنات، جامعة بغداد، بغداد، العراق. saharsabeeh21@yahoo.com

الخلاصة

تم تحضير معقدات المعادن (II) لكل من Co و Ni و Cu و Zn مع مشتق cefdinir $C_{14}H_{13}N_5O_5S_2$ (L) وتشخيصها عن طريق تحليل العناصر CHNS Uv-Vis و FTIR و TGA وتحليل المعادن AA والقابلية المغناطيسية وإجراء قياس التوصيلية. من خلال التحليل وجد ان الليكاند يسلك سلوك ثنائي السن. بالنسبة لمعقد الكوبالت، تم اقتراح الشكل الهندسي رباعي السطوح، بينما تم اقتراح الشكل الهندسي للمعقدات الأخرى التي تحتوي على أيونات النيكل والنحاس والزنك كشكل هندسي ثماني السطوح. تمت دراسة الطريقة التجريبية لمنع تآكل الكربون الصلب في 3.5% كلوريد الصوديوم (NaCl) باستخدام أدوية مشتقات Cefdinir جديدة. أظهرت النتائج أن المركب المعدني كان يحمي من التآكل القوي للكربون الصلب في كلوريد الصوديوم وأن كفاءة التثبيط (IE%) تزداد مع زيادة تركيز الأدوية بسبب أن المركب المعدني الجديد المشتق من Cefdinir هو ممتاز من محلول ملحي على سطح الكربون الصلب.

الكلمات المفتاحية: مقاومة التآكل، تحليل العناصر CHNS، مطيافية Uv-Vis، FTIR، مشتق Cefdinir.

INTRODUCTION

Schiff bases are formed when any primary amine reacts with an aldehyde or a ketone under specific conditions. Structurally, a Schiff base (also known as imine or azomethine) is a nitrogen analogue of an aldehyde or ketone in which the carbonyl group (CO) has been replaced by an imine or azomethine group. Schiff base ligands are easily synthesized and form complexes with almost all metal ions. Over the past few years, there have been many reports on their applications in biology including antibacterial, antifungal, anticancer, antioxidant, anti-inflammatory, antimalarial, antiviral activity and also as catalyst in several reactions such as polymerization reaction, reduction of thionyl chloride, oxidation of organic compounds, reduction reaction of ketones, aldol reaction, Henry reaction, epoxidation of alkenes, hydrosilylation of ketones, synthesis of bis (indolyl) methane's and Diels–Alder reaction, hence the need for a review article highlighting the uses of Schiff base ligands and their complexes. Co-ordination compounds play serious roles in biology, biochemistry, medicine, function of many enzymes, their metabolisms, and also in many industrial processes in the development of new materials with specially designed properties (Yousif *et al.*, 2017; Annapoorani & Krishnan, 2013). Thus, synthesis and study of such complexes are very important. Schiff bases (SB) lodge a main position as ligands in metal co-ordination chemistry owing to their prominence as catalysts in their biological activities (Liu *et al.*, 2018; Yu *et al.*, 2017). Besides macrocyclic derivatives, these SB ligands have countless ultimate purposes like photosynthesis, oxygen transportation in mammals, and further respirational schemes (Gautam *et al.*, 2016; Khalaji *et al.*, 2015). Heteroatoms present in SB ligands show good biological activity in a variety of ways that are coordinated to metal ions. They also epitomize models for metallo-enzymes, which efficiently catalyze the reduction of di-nitrogen and di-oxygen (Yurt *et al.*, 2005). Corrosion is one of the largest problems the planet has, which occurs when a metal returns to its original state and transforms into oxides or hydroxides in a variety of gaseous or aqueous settings. Carbon steel is one of the most commonly corrosive metals. In addition to disrupting pipeline manufacturing processes, low productivity, and delays, corrosion also results in pollution and poses health hazards to the general public (Kadhim *et al.*, 2018). It is required to add elements such as organic, inorganic, or natural chemicals in order to maintain minerals and decrease corrosion processes. These compounds are known as inhibitors, which are substances introduced to liquids or gases in very minute quantities (parts per million), with the purpose of forming a layer of film that covers it, stopping any chemical reactions, and shielding it from any outside impacts (Sowmyashree *et al.*, 2021).

The inorganic mixes have chromate, nitrites and mixes have hetro particles (O, P, S, N), π bonds were best and productive (Ramdé *et al.*, 2016). Mixes containing both nitrogen and chloro molecules may give fantastic hindrance, contrasted and mixes containing just nitrogen or chloro particle (Abboud *et al.*, 2007). Heterocyclic mixes, for example, anti-infection (drug drugs) may give superb restraint. These particles relies principally upon certain actual properties of the inhibitor particle, for example, utilitarian gatherings, steric factors, electron thickness at the contributor iota and electronic structure of the atoms (Popova *et al.*, 2004). A couple of scientists have been accounted for the utilization of antibacterial medications as consumption inhibitors because of that of essence of oxygen, nitrogen and sulfur as well as in their systems dynamic focuses, high solvency in water, high atomic size, non-harmful-environmentally friendlyl erosion inhibitors, significant in organic responses and medications that might be effortlessly created and sanitized (Samide *et al.*, 2011).

The electrochemical system consists of a potentiostat, three electrodes, with a controlled computer and standard corrosion cell. The thermostat was among the most widely,

using to control the temperature of (3.5% NaCl) which is 30 degrees Celsius and flows by the external vessel the corrosion cell, as well as the three electrodes, are depicted in (Figure 1) are:

1. The first is reference electrodes based on its potential consist of AgCl, Ag, KCl, and the outer solution filled with the prepared Sodium Chloride solution (3.5% NaCl). The reference electrode, a lugging tube placed at the distance 2mm from working electrode.
2. The second electrode is auxiliary consist of high purity platinum rod with 0.6 mm in diameter and 10 cm in length.
3. The third is working electrode (Carbon steel) which was mounted in the working electrode load with 1 cm^2 surface area the opening uncovered to the acidic solution.

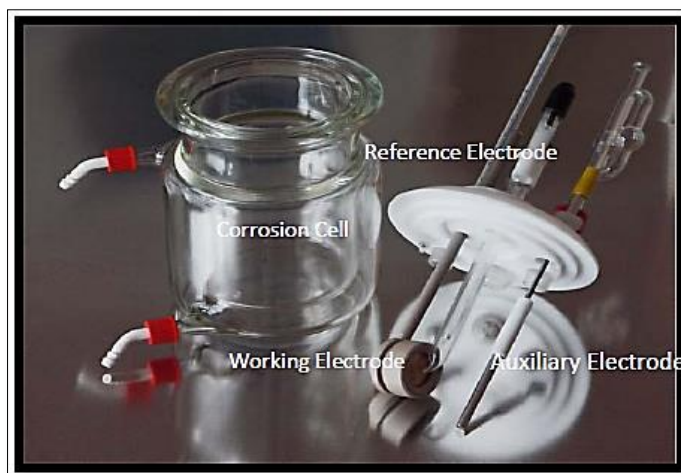


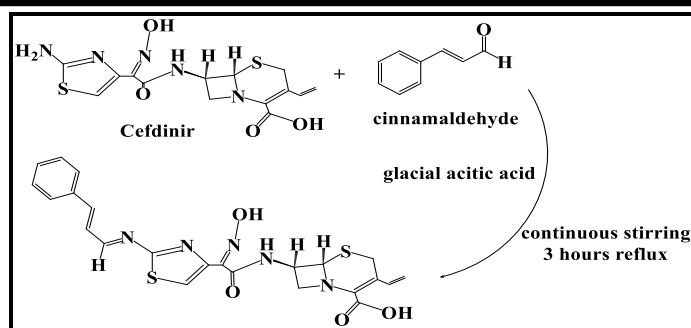
Figure (1): Corrosion cell and three electrode.

MATERIALS AND METHOD

The next chemical materials were obtainable trading products, cefdinir $\text{C}_{14}\text{H}_{13}\text{N}_5\text{O}_5\text{S}_2$, metal salts $\text{CoCl}_2 \cdot 6\text{H}_2\text{O}$, CH_3COOH , $\text{NiCl}_2 \cdot 6\text{H}_2\text{O}$, ZnCl_2 and $(\text{CuCl}_2 \cdot 2\text{H}_2\text{O})$, gained from F-897ewluka, sigma Aldrich. FTIR was detected in the range of $4000\text{-}200 \text{ cm}^{-1}$ with KBr disk and $4000\text{-}200 \text{ cm}^{-1}$ with CsI disk on a Shimadzu-3800 Spectro-meter. The electronic spectral data were detected by using Shimadzu160 Spectro-photometer. Melting point apparatus of Gallencamp MF. B-600.01 was used. Molar Conductivity was used to measure the conductivity of the complexes at room temperature in freshly prepared 10^{-3} M in absolute ethanol using coring conductivity meter 220 (Hassan *et al.*, 2020).

Synthesis of ligand L

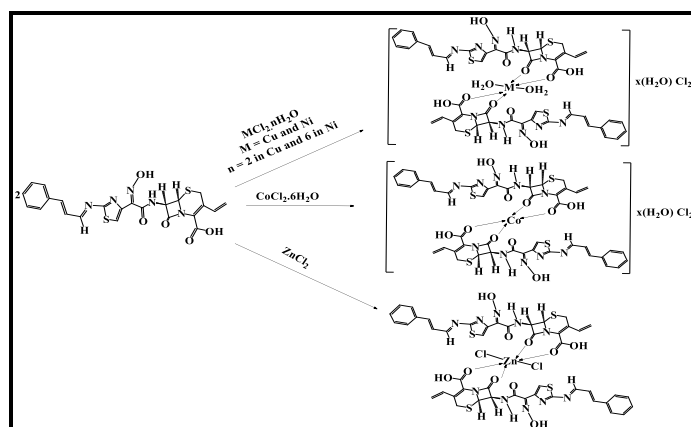
Schiff base in (Scheme 1) was synthesized in round flask 25 mL as volume by dissolving 0.79 g, 0.0019 mol from cefdinir $\text{C}_{14}\text{H}_{13}\text{N}_5\text{O}_5\text{S}_2$ in 5 mL ethanol with continuous stirring, then adding 0.264 g, 0.0019 mol cinnamaldehyde which dissolved in 5 mL ethanol followed by the addition of 3 drops of glacial acetic acid, refluxing for 3 h. a yellow solution is formed then leaving the solution at room temperature to be dried, finally, a yellow precipitate will be gained (Pragathiswaran *et al.*, 2021).



Scheme (1): Synthesis of ligand.

Synthesis of the complexes

were synthesized by the reaction of 0.2 g, 0.0004mol from the ligand $C_{14}H_{13}N_5O_5S_2$ (2 L:1 M) mole ratio with 0.042 g, 0.059 g, 0.059 g and 0.027 g for each of $CuCl_2 \cdot 2H_2O$, $CoCl_2 \cdot 6H_2O$, $NiCl_2 \cdot 6H_2O$ and $ZnCl_2$ metal salts respectively in (scheme 2). The amounts of all metal salts were 0.00024 mol, as show (scheme 2) (Wang, 2001).



Scheme (2): Synthesis of complexes.

RESULT AND DISCUSSION

All physical properties are ill suited in (Table 1), the complexes are characterized with stability at room temperature with various melting points and different colors.

Table (1): Physical properties of the ligand and its complexes.

| Compounds | Elemental analysis Found, (Cal.) % | | | | M.P (°C) | Color | Yield (%) | μscm^{-1} |
|---------------------------------------|---------------------------------------|----------------|------------------|----------------|-------------|-----------------|--------------|----------------------|
| | C | H | N | M | | | | |
| $C_{14}H_{13}N_5O_5S_2$ (L2) | 48.2 (50.0) | 5.01 (5.80) | 18.1 (19.4) | ----- | 190 | Light yellow | 85 | ----- |
| $CoC_{28}H_{26}N_{10}S_4Cl_2$ (Co-L2) | 38.6 (39.4) | 4.53 (5.12) | 14.05 (15.12) | 5.54 (5.71) | 187 | Bluish green | 81 | 50.51 |
| $NiC_{28}H_{26}N_{10}S_4Cl_2$ (Ni-L2) | 39.10 (40.75) | 4.77 (5.02) | 13.08 (14.22) | 4.45 (5.25) | 200 | Light brown | 78 | 41.32 |
| $CuC_{28}H_{26}N_{10}S_4Cl_2$ (Cu-L2) | 41.78 (42.00) | 4.79 (4.04) | 12.71 (13.99) | 5.05 (5.82) | 160 | Olive | 67 | 45.31 |
| $ZnC_{28}H_{26}N_{10}S_4Cl_2$ (Zn-L2) | 39.82 (42.04) | 4.99 (5.08) | 12.35 (13.90) | 5.73 (6.12) | 190 | Light yellow | 80 | 33.64 |

FT-IR studies

Returning to FT-IR spectrum of the synthesized ligand we can notice distinguishable variations in absorption bands between the starting materials and the formed molecule, these variations are, disappearance of the stretching absorption bands of both N-H and C=O groups which belong to starting materials due to the occurrence of imine interaction through these groups, which in turn gives unique stretching absorption band at 1600 cm^{-1} , as demonstrated in (Figure 2). In addition to other absorption bands illustrated in (Table 2) in addition to the appearance of many stretching absorption bands at 3235 cm^{-1} , 3068 cm^{-1} and 2936 cm^{-1} those bands belong to the stretching vibrational modes of N-H amino group, C-H aromatic and C-H aliphatic groups respectively. In FT-IR spectra of the related complexes, (Figure 3) and (Table 2) we can clearly notice the occurrence of coordination through C=O groups of both (β -lactam and carboxylic acid) of the ligand because of the chemical shifting in the stretching absorption bands of C=O (β -lactam) group compared with the same band of the ligand by 5 cm^{-1} , 25 cm^{-1} , 13 cm^{-1} and $-\text{ cm}^{-1}$ for each of Zn, Co, Ni and Cu respectively, to be appeared at 1761, 1741 1753 and $-\text{ cm}^{-1}$ for each of them respectively. In addition to the shifting in the stretching absorption bands of C=O carboxylic group by 3, 5, 7 and 6 cm^{-1} to be appeared at 1670, 1672, 1674 and 1673 cm^{-1} for each of the mentioned metal complexes respectively. Additionally, we can observe some new bands belong to: M-O absorption bands as illustrated in (Table 2) which prove the occurrence of coordination through C=O of both β -lactam and carboxylic acid groups, M-Cl for only Zn-complex and aqua (H_2O) bands (Hassan *et al.*, 2020).

Table (2): FT-IR spectral records of the formers.

| Comp. | N-H | C-H Arom. | C-H Alph. | C=O acid | C=O β -lactam | C=N | H ₂ O | M-O | M-Cl |
|-------|------|-----------|-----------|----------|---------------------|------|------------------|-----|------|
| L2 | 3235 | 3068 | 2936 | 1667 | 1666 | 1600 | 3397 | - | - |
| Zn L2 | 3233 | 3067 | 2933 | 1670 | 1761 | 1600 | 3390 | 482 | 388 |
| Co L2 | 3231 | 3065 | - | 1672 | 1741 | 1602 | 3397 | 400 | 383 |
| Ni L2 | 3234 | 3067 | 2961 | 1674 | 1753 | 1600 | 3390 | 482 | 383 |
| Cu L2 | 3232 | 3060 | 2961 | 1673 | - | 1602 | 3392 | - | 383 |

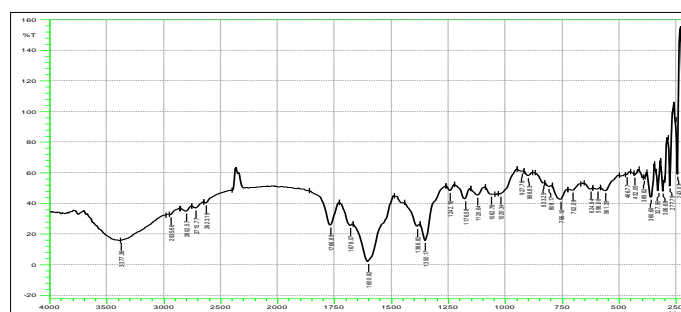


Figure (2): FT-IR spectrum of ligand.

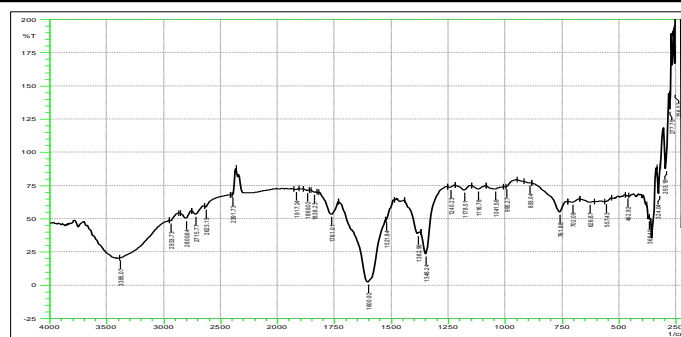


Figure (3): FT-IR spectrum of Zn complex.

UV-Vis studies

When discuss the UV-Vis spectrum (Figure 4) of the ligand we can clearly observe the following electronic transitions $n \rightarrow \pi^*$ because of the presence of hetro atoms in ligand structure and $\pi \rightarrow \pi^*$ at 299 and 222 nm respectively corresponded to 33445 and 45045 cm^{-1} respectively. In the case of UV-Vis spectra (Figure 5) and (Table 3) of its related complexes Co, Ni, Cu and Zn we can also observe the following transitions: ${}^4A_2 \rightarrow {}^4T_{2(F)}$, ${}^4A_2 \rightarrow {}^4T_{1(F)}$ and ${}^4A_2 \rightarrow {}^4T_{1(P)}$ at -, - and 602 nm respectively, corresponded to 3479, 5288 and 16611 cm^{-1} respectively, those transitions supports Td geometry for Co-complex, ${}^3A_2g \rightarrow {}^3T_2g$, ${}^3A_2g \rightarrow {}^3T_{1g(F)}$ and ${}^3A_2g \rightarrow {}^3T_{1g(P)}$ at 898, 638 and 428 nm respectively, corresponded to 11136, 15674 and 23364 cm^{-1} respectively, those transitions supports Oh geometry for Ni complex, ${}^2E_g \rightarrow {}^2T_2g$, and two C.T transitions at 891, 304 and 246 nm respectively, corresponded to 11223, 32895 and 40650 cm^{-1} respectively, those transitions supports Oh geometry for Cu-complex and two C.T transitions at 277 and 203 nm corresponds to 36101 and 49261 cm^{-1} respectively, which support Oh geometry for Zn-complex (Hassan *et al.*, 2021).

Table (3): UV-Vis spectral records of ligand and related complexes.

| Compound | λ_{max} nm | $\bar{\nu}$ cm^{-1} | Assignment | Geometries |
|----------|---------------------------|------------------------------|--------------------------------------|------------|
| L2 | 222 | 45045 | $\pi \rightarrow \pi^*$ | ----- |
| | 299 | 33445 | $n \rightarrow \pi^*$ | |
| Co L2 | - | 3479 | ${}^4A_2 \rightarrow {}^4T_{2(F)}$ | Td |
| | - | 5288 | ${}^4A_2 \rightarrow {}^4T_{1(F)}$ | |
| | 602 | 16611 | ${}^4A_2 \rightarrow {}^4T_{1(P)}$ | |
| Ni L2 | 898 | 11136 | ${}^3A_2g \rightarrow {}^3T_2g$ | Oh |
| | 638 | 15674 | ${}^3A_2g \rightarrow {}^3T_{1g(F)}$ | |
| | 428 | 23364 | ${}^3A_2g \rightarrow {}^3T_{1g(P)}$ | |
| Cu L2 | 891 | 11223 | ${}^2E_g \rightarrow {}^2T_2g$ | Oh |
| | 304 | 32895 | C.T | |
| | 246 | 40650 | C.T | |
| ZnL2 | 277 | 36101 | C.T | Oh |
| | 203 | 49261 | C.T | |

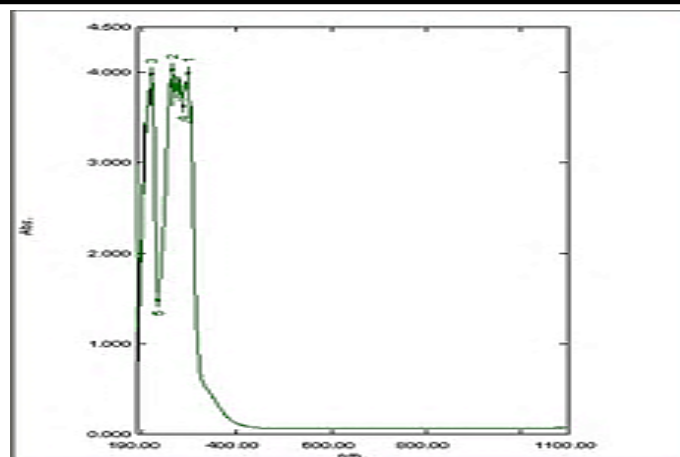


Figure (4): UV-Vis spectrum of ligand.

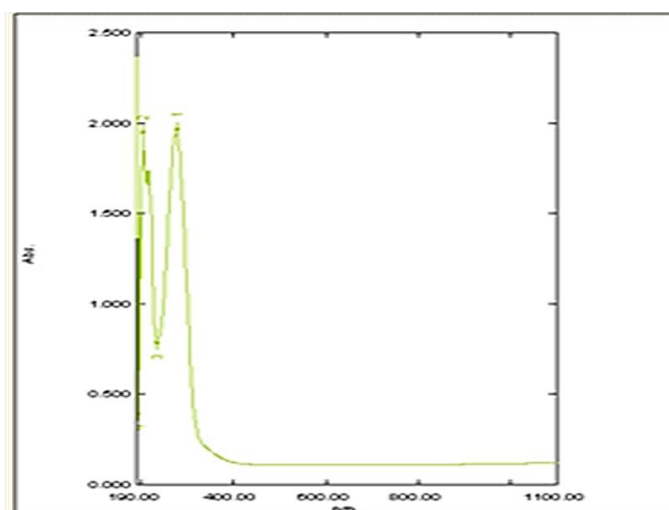


Figure (5): UV-Vis spectrum of Zn-complex.

Thermogravimetric analysis

The study of thermal stability of the synthesized ligand and its complexes using TGA technique, it was noticed that, the complexes were stable and decomposes in four or five steps according to their mass loss as illustrated in (Table, 4) At first step, hydrated water molecules and weight are lost as methyl, carbon monoxide and hydrogen as gasses. The observational mass loss at final steps with increasing in temperature leads to losing chemical bonds in complexes and MO is left behind.

Table (4): TGA steps of the complexes.

| Comp. | Decomposition stage | Temp. range (°C) | Weight loss found (cal) (%) | Decomposition Assignment |
|------------------|---------------------|------------------|-----------------------------|--|
| CoL ₂ | I | 60-151 | 3.26(3.32) | Out of sphere water |
| | II | 151-390 | 11.48(11.51) | 4CH ₃ -2Cl |
| | III | 390-570 | 69.10(70.92) | C ₄₂ H ₂₆ N ₁₀ O ₁₀ S ₄ |
| | IV | >570 | 6.02(6.21) | CoO residue |
| NiL ₂ | I | 65-150 | 2.27(2.45) | Out of sphere water |
| | II | 150-250 | 3.30(3.52) | Coordination water molecule |
| | III | 250-390 | 11.50(11.95) | 2Cl. 4CH ₃ |
| | IV | 390-570 | 72.80(72.12) | C ₄₂ H ₃ ON ₁₀ O ₁₂ S ₄ |
| | V | >610 | 6.22(6.45) | NiO residue |
| CuL ₂ | I | 65-152 | 0.89(0.97) | Out of sphere water |
| | II | 152-250 | 3.21(3.19) | Coordination water molecule |
| | III | 250-390 | 12.18(12.78) | 2Cl. 4CH ₃ |
| | IV | 390-570 | 72.5(71.95) | C ₄₂ H ₃ ON ₁₀ O ₁₂ S ₄ |
| | V | >605 | 7.84(8.14) | CuO residue |
| ZnL ₂ | I | | 3.10(3.47) | Out of sphere water |
| | II | | 11.46(11.98) | 4CH ₃ -2Cl |
| | III | >612 | 71.95(72.01) | C ₄₂ H ₂₆ N ₁₀ O ₁₀ S ₄ |
| | IV | | 6.01(6.17) | ZnO residue |

Potentiostatic polarization measurements

The Potentiostatic Polarization curves for Carbon steel without and with a new (Zn-complex) immersed in 3.5% NaCl solution at temperatures 298 K are show in (Figure 6) and the results are listed in (Table 5).

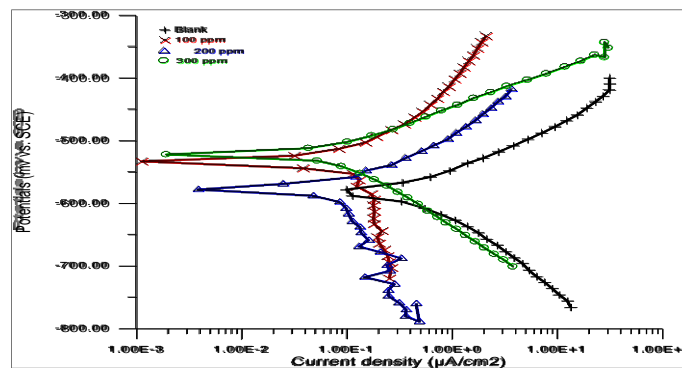


Figure (6): Potentiostatic polarization curves for carbon steel, whether uncoated and coated of metal complexes in 3.5% NaCl Solution at 298 K.

Table (5): Polarization parameters for different concentrations of metal complexes at carbon steel in 3.5% NaCl at 298 K.

| Conc.(mM) | -Ecorr/mV | Icorr./µA.cm ² | ba/mV/Dec | ba/mV/Dec | W.L.g.m ⁻² .d ⁻¹ | P.L mm.y ⁻¹ | Rp/Ω.cm ² | IE (%) | CR mpy |
|-----------|-----------|---------------------------|-----------|-----------|--|------------------------|----------------------|--------|--------|
| 143.61 | 0 | 52.92 | 0.961 | 77.7 | 65.2 | 90.5 | 310.93 | 579.5 | Blank |
| 41.37 | 71.19 | 224.09 | 0.321 | 18 | 79.6 | 110.3 | 89.58 | 522.2 | 100 |
| 34.84 | 75.74 | 257.66 | 0.199 | 15 | 76.4 | 108.1 | 75.43 | 580.5 | 200 |
| 29.61 | 79.38 | 345.01 | 0.131 | 13 | 84.2 | 128.9 | 64.10 | 522.9 | 300 |



Corrosion potential values corrosion current densities, E_{corr} , cathodic and anodic i_{corr} slopes b_c and b_a on the Tafel. R_p polarization resistance which determined by equation (1), CR corrosion rate determined by equation. (2), the inhibition efficiency of a new cefdinir derivative drugs may calculated from equation (3) (Jasim *et al.*, 2020).

$$R_p = \left(\frac{B}{i_{corr}}\right) \dots\dots\dots (1)$$

$$R_p = \frac{\beta_a \beta_c}{2.303 (\beta_a + \beta_c) i_{corr}}$$

$$CR = 0.13 \left(\frac{e}{\rho}\right) i_{corr} \dots\dots\dots (2)$$

e: Chemical equivalent

p: density of mild steel

$$(\%) = \left(\frac{i_{corr} - i_{inh\ corr}}{i_{corr}}\right) \times 100 \dots\dots\dots (3)$$

Where i_{corr} . and $i_{inhcorr}$. The corrosion current density without and with the inhibitor, respectively, is referred to the inhibition efficiency improved as the concentration of the new Cefdinir derivative was increased, owing to the complicated impact of the new Cefdinir derivative on the anodic and cathodic electrochemical corrosion reactions, as a new Cefdinir derivative includes heteroatoms such as nitrogen, sulfur, and oxygen atoms, as well as the planarity (Wang, 2001). the inhibition resistance increases as the inhibitor concentration increases is due the inhibitor binds to the metal surface and forms a double layer of film, which reduces the rate of corrosion. It is the most efficient anti-corrosion at 300 ppm and 25°C (Pragathiswaran *et al.*, 2021).

Effect of (complexes+ Zn) concentration

The addition of ((Complexes+ Zn)) to carbon steel in 3.5% NaCl at 25°C decreases the corrosion rates as shown in (Table 6). these results decrease as the concentration of inhibitor is changed towards higher side revealing the fact that the adsorption of inhibitor and surface coverage metal increase with increasing the inhibitor concentration (Naqvi *et al.*, 2011).

Table (6): The values of corrosion rates, inhibition efficiency IE(%) and (θ) surface coverage degree for carbon steel corrosion in without and with addition of different concentrations of (Complexes+Zn) in 3.5% NaCl solution at 25°C.

| Inhibitor Con. (ppm) | Temp. (°C) | Corrosion rate (g/m ² .d) | Surface coverage degree (θ) | Inhibition Efficiency (IE) (%) |
|----------------------|------------|--------------------------------------|-----------------------------|--------------------------------|
| Blank | 25 | 143.61 | 0.00 | 0.00 |
| (Complexes + Zn) | | | | |
| 100 | 25 | 41.37 | 0.7119 | 71.19 |
| 200 | | 34.84 | 0.7574 | 75.74 |
| 300 | | 29.61 | 0.7938 | 79.38 |

CONCLUSION

The use of a Cefdinir derivative could to protect the metal carbon steel dissolution in NaCl solution is by using (Complex Zn) using potentiodynamic polarization, and weight loss through blocking influence by the adsorption of inhibitor molecules on the carbon steel surface.

REFERENCES

1. Abboud, Y., Abourriche, A., Saffaj, T., Berrada, M., Charrouf, M., Bennamara, A. & Hannache, H. (2007). 2, 3-Quinoxalinedione as a novel corrosion inhibitor for mild steel in 1 M HCl. *Materials Chemistry and Physics*, 105(1), 1-5.
2. Annapoorani, S. & Krishnan, C. (2013). Synthesis and spectroscopic studies of trinuclear N4 Schiff base complexes international, *International Journal of Chemtech Research*, 5(1), 180-185.
3. Gautam, A. K., Kumar, A., Sharma, K. & Rai, B. (2016). Synthesis and structural characterization of Schiff base ligand and their metal complexes. *Oriental Journal of Chemistry*, 32, 1249-1254.
4. Hassan, S. S., Hassan, N. M., Baqer, S. R. & Saleh, A. M. (2021). Biological evaluation and theoretical study of bi-dentate ligand for amoxicillin derivative with some metal ions. *Baghdad Science Journal*, 18(4), 1269-1269.
5. Hassan, S. S., Hassan, N. M., Kadhim, N. J. & Abd, Z. N. (2020). Synthesis, characterization, theoretical study and biological activity of Schiff base metal complexes derived from cefotaxime with 5, 5-diethyl-6-iminodihydropyrimidine-2, 4 (1H, 3H)-dione. *International Journal of Pharmaceutical Research*, 12(4), 67-75.
6. Jasim, R. A., Kadhim, N. J., Farhan, A. M. & Hadi, M. S. (2020). *Nano-Particals as corrosion inhibitors for Aluminum alloys in acidic solution at different Temperatures*. Paper presented at the IOP Conference Series: Materials Science and Engineering. volume 928, 2nd International scientific conference of Al-Ayen university (ISCAU-2020) 15-16 July 2020, Thi-Qar, Iraq.
7. Kadhim, N. J., Farhan, A. M. & Jaafer, H. I. (2018). Anticorrosion behavior of deposited magnetite on galvanized steel in saline water using RF-magnetron sputtering. *Baghdad Science Journal*, 15(4), 34-46.
8. Khalaji, A., Hafez, G. S., Pojarová, M. & Dušek, M. (2015). Characterization and crystal structures of new Schiff base macrocyclic compounds. *Journal of Structural Chemistry*, 56(7), 1410-1414.
9. Liu, Y. T., Sheng, J., Yin, D. W., Xin, H., Yang, X. M., Qiao, Q. Y. & Yang, Z. J. (2018). Ferrocenyl chalcone-based Schiff bases and their metal complexes: Highly efficient, solvent-free synthesis, characterization, biological research. *Journal of Organometallic Chemistry*, 856, 27-33.
10. Naqvi, I., Saleemi, A. & Naveed, S. (2011). Cefixime: a drug as efficient corrosion inhibitor for mild steel in acidic media. *International Journal of Electrochemical Science*, 6(1), 146-161.
11. Popova, A., Christov, M., Raicheva, S. & Sokolova, E. (2004). Adsorption and inhibitive properties of benzimidazole derivatives in acid mild steel corrosion. *Corrosion Science*, 46(6), 1333-1350.
12. Pragathiswaran, C., Ramadevi, P. & Kumar, K. K. (2021). Imidazole and Al nano material as corrosion inhibitor for mild steel in hydrochloric acid solutions. *Materials Today: Proceedings*, 37, 2912-2916.
13. Ramdé, T., Rossi, S. & Bonou, L. (2016). Corrosion inhibition action of sulfamethoxazole for brass in acidic media. *International Journal of Electrochemical Science*, 11, 6819-6829.
14. Samide, A., Tutunaru, B. & Negrila, C. (2011). Corrosion inhibition of carbon steel in hydrochloric acid solution using a sulfa drug. *Chemical and Biochemical Engineering Quarterly*, 25(3), 299-308.



15. Sowmyashree, A., Somya, A., Kumar, C. P. & Rao, S. (2021). Novel nano corrosion inhibitor, integrated zinc titanate nano particles: Synthesis, characterization, thermodynamic and electrochemical studies. *Journal of Surfaces and Interfaces of Materials*, 22, 100812.
16. Wang, L. (2001). Inhibiting effect of 2-mercaptopyrimidine on the corrosion of a low carbon steel in phosphoric acid. *Corrosion Science*, 43(9), 1637-1644.
17. Yousif, E., Majeed, A., Al-Sammarrae, K., Salih, N., Salimon, J. & Abdullah, B. (2017). Metal complexes of Schiff base: preparation, characterization and antibacterial activity. *Arabian Journal of Chemistry*, 10, S1639-S1644.
18. Yu, H., Zhang, W., Yu, Q., Huang, F. P., Bian, H. D. & Liang, H. (2017). Ni (II) Complexes with Schiff base ligands: preparation, characterization, DNA/protein interaction and cytotoxicity studies. *Molecules*, 22(10), 1772.
19. Yurt, A., Bereket, G., Kivrak, A., Balaban, A. & Erk, B. (2005). Effect of Schiff bases containing pyridyl group as corrosion inhibitors for low carbon steel in 0.1 M HCl. *Journal of Applied Electrochemistry*, 35(10), 1025-1032.